J Mater Sci: Mater Med (2009) 20:2117–2128
DOI 10.1007/s10856-009-3766-5

Bioactivated collagen-based scaffolds embedding protein-releasing biodegradable microspheres: tuning of protein release kinetics

Marco Biondi · Laura Indolfi · Francesca Ungaro · Fabiana Quaglia · Maria Immacolata La Rotonda · Paolo A. Netti

Received: 20 February 2009 / Accepted: 24 April 2009 / Published online: 18 May 2009

Abstract In tissue engineering, the recapitulation of natural sequences of signaling molecules, such as growth factors, as occurring in the native extracellular matrix (ECM), is fundamental to support the stepwise process of tissue regeneration. Among the manifold of tissue engineering strategies, a promising one is based on the creation of the chrono-programmed presentation of different signaling proteins. This approach is based upon the integration of biodegradable microspheres, loaded with suitable protein molecules, within scaffolds made of collagen and, in case, hyaluronic acid, which are two of the fundamental ECM constituents. However, for the design of bioactivated gel-like scaffolds the determination of release kinetics must be performed directly within the tissue engineering template. In this work, biodegradable poly(lactic-co-glycolic)acid (PLGA) microspheres were produced by the multiple emulsion-solvent evaporation technique and loaded with rhodamine-labelled bovine serum albumin (BSA-Rhod), a fluorescent model protein. The microdevices were dispersed in collagen gels and collagen-hyaluronic acid (HA) semi-interpenetrating networks (semi-IPNs). BSA-Rhod release kinetics were studied directly on single microspheres through confocal laser scanning microscopy (CLSM). To thoroughly investigate the mechanisms governing protein release from PLGA microspheres in gels, BSA-Rhod diffusion in gels was determined by fluorescence correlation spectroscopy (FCS), and water transport through the microsphere bulk was determined by dynamic vapor sorption (DVS). Moreover, the decrease of PLGA molecular weight and glass transition temperature (T_g) were determined by gel permeation chromatography (GPC) and differential scanning calorimetry (DSC), respectively. Results indicate that protein release kinetics and delivery onset strongly depend on the complex interplay between protein transport through the PLGA matrix and in the collagen-based release media, and water sequestration within the scaffolds, related to the scaffold hydrophilicity, which is dictated by HA content. The proper manipulation of all these features may thus allow the obtainment of a fine control over protein sequential delivery and release kinetics within tissue-engineering scaffolds.

M. Biondi · L. Indolfi · F. Ungaro · F. Quaglia · M. I. La Rotonda · P. A. Netti (✉)
Interdisciplinary Research Centre on Biomaterials (CRIB), University of Naples Federico II, 80125 Naples, Italy
e-mail: nettipa@unina.it

M. Biondi · L. Indolfi · F. Ungaro · F. Quaglia · M. I. La Rotonda · P. A. Netti
Italian Institute of Technology (IIT), via Morego 30, 16163 Genoa, Italy

1 Introduction

Ideal scaffolds for tissue engineering should provide spatial confinement to the ingrowing tissue as well as exert an active control over the cellular events, namely attachment, migration, proliferation and differentiation, occurring during tissue regrowth [1–3]. This could be realized by a continuous sequestration and chrono-programmed delivery of signaling molecules, such as growth factors, according to known sequential patterns with the aim of recapitulating the cascade of morphogenetic factors stimulating the regrowth of the highly organized structures of complex tissues. In particular, the regenerative capability of a scaffold strongly relies upon the engineered, chrono-

programmed delivery of growth factors [4–6]. Indeed, growth factors must be released locally and for long times (days to weeks) to prevent their enzymatic deactivation and diffusion out of the target site [7, 8]. Thus, bioactive scaffolds able to provide the prolonged and/or sequential release of growth factors are promising to control cellular behaviours and build functional neo-tissues. In this perspective, tissue engineering is considered a particular case of controlled delivery aiming to control the presentation of morphogenetic factors [6, 8–11].

Scaffolds made of collagen and hyaluronic acid (HA) are attractive as tissue equivalents because both components are fundamental constituents of native extracellular matrix (ECM). Collagen is a fibrillar protein playing a main role in cell–ECM interactions, fibroblast activation and tissue morphogenesis [12, 13], while HA is a main constituent of loose connective tissues involved in the transport of metabolites/nutrients, tissue morphogenesis and molecular signaling [14, 15]. We have recently demonstrated that the integration of protein-releasing microdepots within collagen and collagen-HA scaffolds may enable the tuning of protein release kinetics by properly modifying microsphere formulation and scaffold composition [16]. The aim of this work was to elucidate the multiple transport phenomena governing protein release kinetics from biodegradable poly(lactic-co-glycolic acid) (PLGA) microspheres integrated within collagen-based scaffolds. To this end, a model protein, rhodamine-labelled bovine serum albumin (BSA-Rhod), was encapsulated in different PLGA microsphere formulations, which were dispersed in collagen gels and collagen-HA semi-interpenetrating networks (semi-IPNs) [17] to obtain scaffolds in which the dispersed microdevices act as single point sources of the signaling molecule. Release kinetics from microspheres were studied directly in the scaffolds at the single microsphere level by confocal laser scanning microscopy (CLSM) through the quantification of microsphere unloading. Furthermore, the transport of water inside microspheres and of the protein within the gels was evaluated by dynamic vapor sorption and fluorescence correlation spectroscopy, respectively. Finally, the temporal trends of T_g and molecular weight of microsphere in solution were assessed by differential scanning calorimetry (DSC) and gel permeation chromatography (GPC).

2 Materials and methods

2.1 Materials

Uncapped poly(D,L-lactide-co-glycolide) (PLGA) (Resomer® RG 504 H; lactide/glycolide ratio 50:50 Mw 41.9 kDa; inherent viscosity 0.5 dl/g) was purchased from Boehringer Ingelheim (Germany). Rhodamine-labelled bovine serum albumin (BSA-Rhod; Mw 66 kDa) and rhodamine (Rh6G) were obtained by Molecular Probes Europe BV (The Netherlands). Analytical grade methylene chloride and hydrochloric acid were provided by Carlo Erba (Italy). Poly(vinyl alcohol) (PVA, Mowiol® 40–88), tetrahydrofuran (THF), polystyrene standards for GPC calibration and sodium hydroxide were purchased from Sigma Aldrich (USA). Type I collagen (Vitrogen®; 3.0 mg/ml; pH 2; Nutacon, The Netherlands), hyaluronic acid (HA) (Mw 155 kDa; initial concentration 10 mg/ml; Fidia Advanced Biopolymers, Italy) and Phenol red-free Dulbecco's Modified Eagles Medium (DMEM, Hyclone, Germany) were used.

2.2 Microsphere preparation and characterization

PLGA microspheres encapsulating BSA-Rhod at the theoretical loading of 0.25% (0.25 mg of BSA-Rhod per 100 mg of microspheres) were produced by the double emulsion-solvent evaporation technique as previously reported [16]. Briefly, BSA-Rhod was dissolved in 0.30 ml of water and poured into 3.0 ml of a PLGA solution in methylene chloride (10–15–20% w/v, respectively, corresponding to formulations PLGA10, PLGA15 and PLGA20). The primary emulsion was generated by a high-speed homogenizer (Diax 900 equipped with a tool 6G, Heidolph, Germany) operating at 15,000 rpm for 2 min. The double emulsion was formed by adding the primary emulsion to 30 ml of 0.5% (w/v) aqueous PVA and homogenizing for 1 min at 8,000 rpm (tool 10F). The organic solvent was removed by evaporation under magnetic stirring for 3 h at room temperature (MR 3001K, Heidolph, Germany). Subsequently, the hardened microspheres were washed 3 times with distilled water by centrifugation at 9,000 rpm (Universal 16R, Hettich Zentrifugen, Germany), lyophilized for 24 h at 0.01 atm and −60°C (Modulyo, Edwards, UK). Triplicate batches of each formulation were produced and stored at −20°C until use.

Scanning electron microscopy (SEM) (Leica S440, Germany) was employed to analyze microsphere external shape and morphology after production. The samples were prepared by gold-sputtering under vacuum. Laser light scattering (Coulter LS 100Q, USA; $\lambda = 750$ nm) on a dispersion of freeze-dried microspheres in 0.5% w/v aqueous PVA enabled the determination of microsphere mean volume diameter and size distribution. Analyses were performed in triplicate.

The actual loading of BSA-Rhod in microspheres was determined by dissolving microparticles in 0.5 N NaOH (0.5% w/v) under stirring for 24 h. Samples were centrifuged at 5,000 rpm and 4°C and then analyzed by

spectrofluorometric detection (LS 55 Luminescence spectrometer, PerkinElmer, USA) performed in 96-well white flat-bottom plates (BD Falcon™, Becton, Dickinson & Co., USA) after centrifugation of the solution at 4°C (5,000 rpm) ($\lambda_{ex} = 553$ nm; $\lambda_{em} = 577$ nm. The slits were 5 and 8 nm for excitation and emission, respectively). The relation between fluorescence and concentration was linear in the 0.25–10.0 μg/ml concentration range ($r^2 > 0.98$). Results were averaged over three batches.

Protein distribution within the microspheres was studied through CLSM (LSM 510 Zeiss confocal inverted microscope; Zeiss 20X/3 objective lens; Carl Zeiss, Germany; $\lambda_{ex} = 543$ nm; $\lambda_{em} = 572$ nm) by visualizing equatorial cross-sections of microspheres.

2.3 Kinetics of water absorption in microspheres

Water uptake in microspheres was gravimetrically measured by dynamic vapor sorption analysis carried out in inert nitrogen atmosphere through a high-sensitivity electronic microbalance (resolution: 10^{-8} g), comprising a humidity chamber in which the sample is lodged (Q5000 Sorption analyzer, TA Instruments, USA). Known amounts of microspheres (approximately 20 mg) were placed on the microbalance pan and pre-programmed trends of water activity were superimposed. First, in the drying phase, the samples were placed in 0% relative humidity until a constant weight was reached (13.9 ± 0.3 h). The succeeding sorption phase was carried out by increasing relative humidity (RH) from 0 to 90% (step 10%). At each step, mass increase was recorded as a function of time up to a plateau weight. Sorption isotherms as a function of time were built from water content at equilibrium. All tests were performed in triplicate at 37°C.

2.4 Degradation studies

Morphological variations occurring during microsphere degradation were studied by suspending the devices in phosphate buffer saline solution (PBS, containing 120 mM NaCl, 2.7 mM KCl, 10 mM phosphate salts; pH = 7.4) and incubating the suspensions at 37°C on an undulating rocker platform (15 rpm) (Stovall LifeScience Inc., USA). At scheduled time intervals, microspheres were centrifuged, washed 3 times, lyophilized and analyzed by SEM as described in Sect. 2.2. PLGA microsphere degradation studies were performed on ultra-dilute particle suspensions (0.01% w/v) in PBS incubated at 37°C on a rocker platform under gentle agitation (15 rpm) (Stovall LifeScience Inc., USA). At scheduled time intervals, microsphere suspensions were washed 3 times and freeze-dried. The lyophilized product was dissolved in THF (approximately 0.6% w/v) and 40 μl-samples analyzed by gel permeation chromatography (GPC) to assess the evolution of PLGA molecular weight distributions over time. GPC analysis was performed by a high-performance liquid chromatograph system from Shimadzu (Japan) consisting of a LC-10ADvp solvent delivery module equipped with a Rheodyne® syringe loading sample injector (model 7725i), a RID-10A refractive index detector and a SCL-10Avp system controller. A CLASS-VP software for Windows (Shimadzu, Japan) was used to acquire instrument data. As a stationary phase, two Phenogel® columns (300 × 7.8 mm) (Phenomenex, USA) with pore sizes of 500 and 5000 Å (molecular weight range 0–10,000 KDa, respectively) were used in series. The mobile phase was tetrahydrofuran (THF) at a flow rate of 1 ml/min. The columns were calibrated with polystyrene standards with narrow molecular weight distribution ranging from 400 to 70,000 Da. Natural logarithm of molecular weight was found to be dependent on retention time according to a quadratic law (correlation factor: 0.999). Results are expressed as the natural logarithm of weight-average and number-average molecular weight as a function of time, as obtained from the average on three batches. PLGA is known to undergo pseudo-first order degradation kinetics. Thus, molecular weight data were fitted to the following equations:

$$\begin{cases} \ln[M_w(t)] = \ln[M_{w,0}] - k_{\circ,w}t \\ \ln[M_n(t)] = \ln[M_{n,0}] - k_{\circ,n}t \end{cases} \quad (1)$$

where $M_w(t)$ and $M_n(t)$ are, respectively, weight-average and number-average molecular weights, expressed in Dalton, at time t, $M_{w,0}$ and $M_{n,0}$ weight-average and number-average molecular weights at time zero, $k_{\circ,w}$ and $k_{\circ,n}$ the degradation rate constant of the polymer referred to weight-average and number-average molecular weights [day^{-1}].

2.5 Determination of glass transition temperature

The temporal trends of the glass transition temperature T_g were determined by differential scanning calorimetry (DSC) (modulated DSC TA 2920 Instruments) under a constant nitrogen flow of 100 cm^3/min. Microspheres were placed in an incubator at 37°C for degradation studies (as described in Sect. 2.4). At predetermined time points, the suspensions were washed 3 times, centrifuged and the microspheres lyophilized. Approximately 10 mg of partially degraded microspheres were placed in sealed aluminum pans and dynamic DSC tests carried out (temperature range: 10–80°C; heating rate: 5°C/min; two heating cycles).

2.6 Release kinetics of BSA-Rhod in microsphere-integrated collagen scaffolds

Release kinetics in gels were studied by CLSM as previously described [16]. Collagen scaffolds were prepared by diluting collagen with phenol-red free DMEM to a final collagen concentration of 1.2 mg/ml (Coll1.2 scaffold). The pH was adjusted to 7.4 ± 0.2, and, when employed, hyaluronic acid (HA) was added at 2.5 and 5.0 mg/ml (CollHA2.5 and CollHA5.0 scaffolds, respectively). Microspheres were placed in non-gelled collagen (0.01% w/v) and loaded in microslides (VitroCom Inc., USA) which were incubated at 37°C to induce collagen fibrillogenesis (30 min) and the subsequent BSA-Rhod release. At scheduled time intervals, triplicate samples for each time point were collected and analyzed by CLSM.

For release studies, CLSM settings (laser power, pinhole aperture, detector gain and amplifier offset) were optimized at time zero after 30 single microsphere observations, and were kept constant during the entire release phase. The effect of microsphere position in the observation plane could be neglected because the instrumental error due to the virtual reconstruction of the real image is regulated by the Point Spread Function (PSF), which is invariant under translation [18]. To assess the fluorescence–concentration relation of the protein, standard aqueous BSA-Rhod solutions (0.2–2.0 mg/ml) were prepared, loaded in microslides and analyzed by CLSM with optimized settings. A linear response ($r^2 > 0.99$) was found at each detector gain used for release studies. Protein release kinetics were determined by deriving fluorescence intensity in the equatorial planes of microspheres at scheduled time intervals, and by monitoring the decrease of average fluorescence and correlating it with BSA-Rhod depletion within the microsphere.

Mean fluorescence intensities at time zero, $\overline{\phi}_0$ and at different time points, $\overline{\phi}(t)$, were determined and averaged on 30 microspheres. The linear dependence of fluorescence intensity on protein concentration in fluid phase suggested that the time-dependent dimensionless BSA-Rhod concentration in microspheres, $\gamma(t)$, could be identified with time-dependent ratio of fluorescence intensities as follows:

$$\gamma(t) = \frac{C_{BSA}(t)}{C^0_{BSA}} = \frac{\overline{\phi}(t)}{\overline{\phi}_0}, \tag{2}$$

where $C_{BSA}(t)$ and C^0_{BSA} are BSA-Rhod concentrations in microspheres at time t and time zero, respectively. Release percentage is immediately obtained ($R_{\%} = 100[1 - \gamma(t)]$). The absence of photobleaching on BSA-Rhod in microspheres was ascertained by exposing the microspheres to the laser at maximum power and for times much longer than observation times, and no fluorescence loss was observed under these conditions. Since tetramethylrhodamine is known to be a pH-insensitive dye [19], no fluorescence loss could be correlated to the pH drop occurring within microspheres during PLGA degradation. Therefore, fluorescence decrease was ascribed only to BSA-Rhod release from microspheres. Release data were fitted by a phenomenological equation, in which the rate of variation of BSA-Rhod dimensionless concentration in microspheres is assumed to be proportional to the residual BSA-Rhod fraction according to a kinetic constant, k. The equation also accounts for both an incomplete and delayed release:

$$\frac{d\gamma}{dt} = -k(\gamma - \gamma_\infty)H(t - t_L), \tag{3}$$

where t is the time [day], k the overall kinetic constant [day^{-1}], γ the dimensionless BSA-Rhod concentration in microspheres, γ_∞ the unreleased BSA-Rhod fraction in the experimental time frame, H the Heaviside function and t_L the lag time [day].

2.7 Diffusion studies of BSA-Rhod

Fluorescence correlation spectroscopy (FCS) in combination with CLSM was employed to determine transport properties of BSA-Rhod in collagen-based gels. The method is based on the count of spontaneous fluctuations of the emitted fluorescent light, which correspond, in absence of chemical reaction, to the diffusion of fluorescent species in a very small volume of the sample (order of magnitude: femtoliter). Protein concentration in the gels was optimized at 0.44 μM. Samples of 200 µl of protein-loaded pre-gels (0.44 μM) were poured in 8-well coverglasses (Lab-Tek, Germany), incubated at 37°C and analyzed by FCS after collagen fibrillogenesis (about 30 min). A Zeiss 40× Apochromat water-immersion objective (Carl Zeiss, Germany) was used and laser power was set at 7% in all FCS experiments ($\lambda_{ex} = 514$ nm). Protein transport was studied by observing the spontaneous molecular fluctuations derived from Brownian motion. Transport parameters were derived from the normalized autocorrelation function [20]:

$$G(\tau) = \frac{\langle F(t)F(t+\tau)\rangle}{\langle F(t)\rangle^2} = \frac{\langle \delta F(t)\delta F(t+\tau)\rangle}{\langle F(t)\rangle^2} + 1. \tag{4}$$

Autocorrelation describes the time-dependent tiny fluctuations of fluorescence intensity, $\delta F(t) = F(t) - \langle F(t)\rangle$ and $\delta F(t+\tau) = F(t+\tau) - \langle F(t+\tau)\rangle$ around the mean values $\langle F(t)\rangle$ and $\langle F(t+\tau)\rangle$, respectively.

The autocorrelation function provides information on the dwell time, τ_D, in the control volume [21], which is a prolate spheroid having axes ω_{xy} and ω_z, with a variable structure parameter $S = \omega_z/\omega_{xy}$. The diffusion coefficient was calculated as follows: (i) it was assumed that the control volume is determined by the confocal parameters

(i.e. pinhole aperture, laser power) and the nature of the fluorescent dye only; (ii) the confocal volume was calculated taking into account the well-known diffusion coefficient of rhodamine (2.8×10^{-6} cm^2/s at room temperature [22]) and that it is $\omega_{xy} = \sqrt{4D_{Rhod}\tau_{D,Rhod}}$, where D_{Rhod} is rhodamine diffusion coefficient and $\tau_{D,Rhod}$ the residence time of the diffusing species in the confocal volume, as determined by FCS. After calibration of FCS on standard rhodamine solutions (0.418–2.09 μM), the confocal volume is immediately calculated:

$$V_{conf} = \frac{4\pi}{3} S\omega_{xy}^3; \quad (5)$$

(iii) dwell times of BSA-Rhod in the detection volume were used to calculate the diffusion coefficient of BSA-Rhod, after allowing the gel to reach thermal equilibrium with the surrounding environment, from:

$$D_{BSA-Rhod} = \frac{\omega_{xy}^2}{4\tau_{D,BSA-Rhod}}, \quad (6)$$

where $D_{BSA-Rhod}$and $\tau_{D,BSA-Rhod}$ are, respectively, diffusion coefficient and dwell time in the control volume of BSA-Rhod.

3 Results

3.1 Microsphere properties

As previously reported [16], the adopted formulation conditions allowed to achieve homogeneously distributed microspheres, with a mean diameter around 20 μm, able to encapsulate BSA-Rhod with high efficiency (≥93% for all formulations). Just after production, all microspheres were spherical and possessed a smooth and non porous surface (Fig. 1). On the contrary, SEM images obtained from partially degraded particles showed that after 15 days of incubation microspheres start losing their spherical shape and, after 30 days, total loss of structural integrity occurs (images not shown).

3.2 Water absorption in microspheres

Water transport through the bulk of microspheres was studied through DVS by performing isothermal experiments at 37°C. Table 1 displays that the amount of absorbed water as a function of RH was not dependent on microsphere formulation, being variable between 1.42% and 1.44% of the dry microsphere mass at equilibrium, with 90% RH. Moreover, the kinetics of water absorption were assessed by correlating sample weight increase with time. Weight increase was found to be linearly dependent on time ($r^2 > 0.99$ for all formulations), while the time necessary to reach equilibrium at 90% RH ranged between 303 and 310 min, irrespective of microsphere formulations.

3.3 Microsphere degradation studies

Degradation kinetics were studied as a function of microsphere formulation. The time trends of the logarithm of number-average and weight-average molecular weight for each formulation are plotted in Fig. 2, and the corresponding kinetics constants shown in Table 2. Degradation starts immediately after the incubation in the release medium and, in all cases, a good agreement between experimental data and an exponential fitting function was found until day 35. For longer times (42 and 58 days) bimodal molecular weight distributions were detected (data not shown).

Changes in the T_g of the polymer after exposure to the release medium are reported in Fig. 3. For all formulations, a sigmoidal trend of the drop of T_g was observed, and the trends were substantially the same irrespective of microsphere formulation. T_g was found out to be basically constant until day 14 (approximately 43–48°C), while a relatively rapid drop in the temperature was observed afterwards to about 28°C after 30–35 days of release.

3.4 Release kinetics of BSA-Rhod in microsphere-integrated collagen-based scaffolds

In vitro release profiles of BSA-Rhod from microspheres, as assessed through CLSM-based technique in different collagen-based scaffolds and from different microsphere formulations, are reported in Fig. 4. The corresponding kinetic parameters as calculated by Eq. 4 are listed in Table 3. Independently from the collagen scaffold embedding the microspheres, it was found that the formulation strongly influences release kinetics. In fact, PLGA10 formulation evidenced an immediate, two-step release characterized by a significant initial burst effect followed by a slower release stage. In the case of PLGA15 and PLGA20 formulations a t_L (time-lag), increasing with increasing polymer concentration in the organic phase of the emulsion, was found. The effect of scaffold composition on BSA-Rhod release kinetics was evaluated for all formulations in collagen/HA semi-IPNs. Release data also showed that HA plays an important role in determining BSA-Rhod release kinetics. In the case of PLGA10, HA addition within the scaffold induced a progressive drop of release rate as evidenced by the reduction of the kinetic constant k. For PLGA15 and PLGA20, k was found to be basically independent on HA concentration, which has a prominent effect on the release onset delay (Table 3).

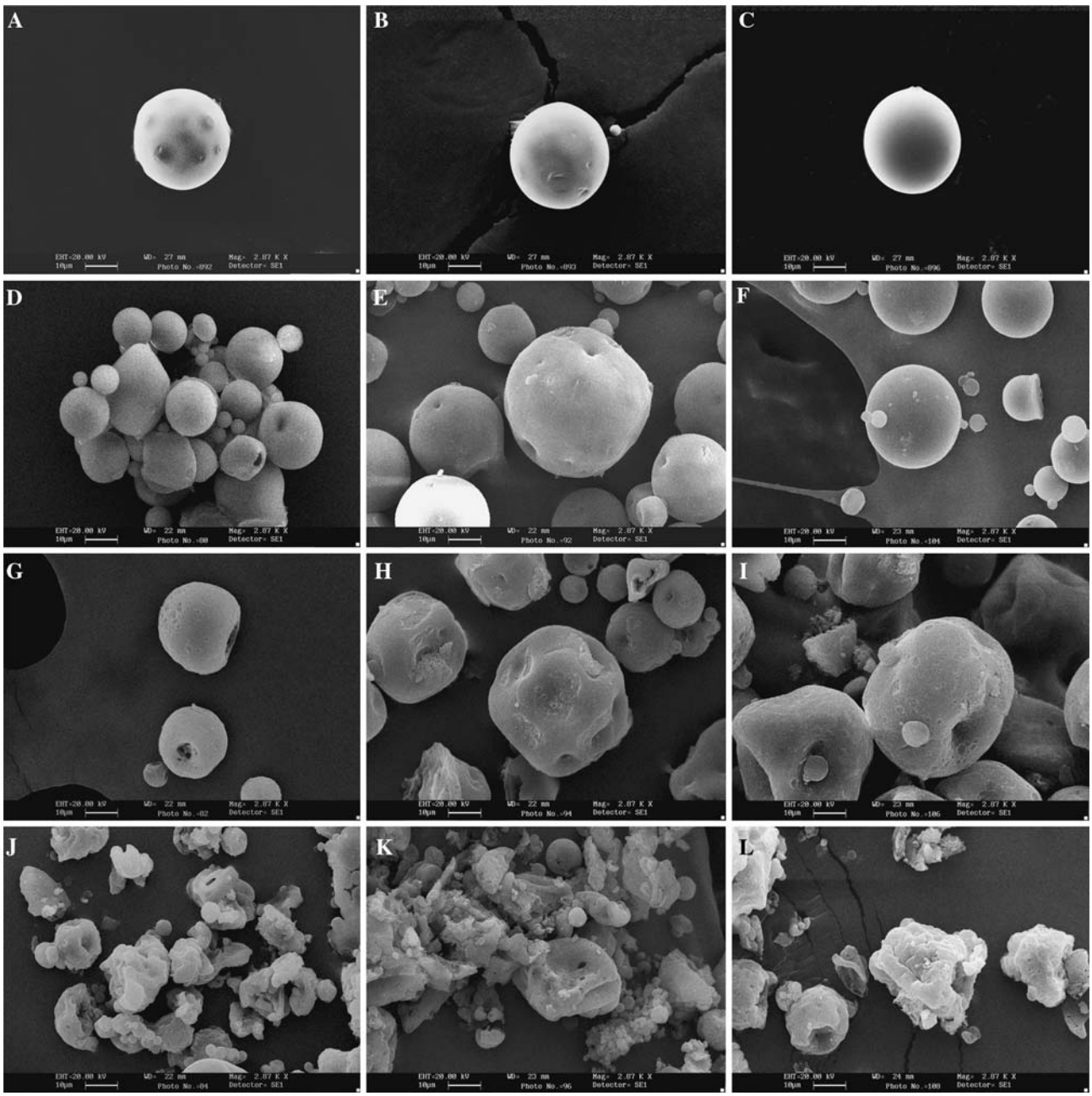

Fig. 1 SEM images of microspheres at time 0 (**a**–**c**) and degrading microspheres after 8 (**d**–**f**), 15 (**g**–**i**) and 21 (**j**–**l**) days of degradation. Microsphere formulations: PLGA10 (**a**, **d**, **g**, **j**), PLGA15 (**b**, **e**, **h**, **k**), PLGA20 (**c**, **f**, **i**, **l**)

3.5 BSA-Rhod diffusion in collagen-based scaffolds

The effect of release environment on BSA-Rhod transport properties was evaluated by measuring BSA-Rhod diffusion coefficients ($D_{BSA-Rhod}$) in collagen and collagen/HA semi-IPNs. Structure parameters were found to range between 7.6 and 10.8 in all experiments. The presence of HA within collagen scaffolds was demonstrated to induce a significant reduction of $D_{BSA-Rhod}$, with values ranging between 4.39×10^{-7} (in collagen) and 2.42×10^{-7} cm^2/s in CollHA5.0 (Table 3).

4 Discussion

In our previous work, protein-loaded PLGA microspheres were integrated within collagen-based gels with the aim to obtain bioactivated scaffolds for tissue engineering [16].

Table 1 DVS results. Percentage of mass variations and the corresponding time point

RH[a] (%)	PLGA10		PLGA15		PLGA20	
	t ± SD[b] (min)	Δm[c] ± SD[b] (%)	t ± SD[b] (min)	Δm[c] ± SD[b] (%)	t ± SD[b] (min)	Δm[c] ± SD (%)
0	0	0	0	0	0	0
10	30.0 ± 0.3	0.093 ± 0.007	31.0 ± 1.4	0.093 ± 0.007	30.6 ± 1.7	0.088 ± 0.002
20	67.5 ± 10.6	0.199 ± 0.006	68.9 ± 13.2	0.201 ± 0.003	76.4 ± 3.2	0.197 ± 0.008
30	82.5 ± 10.3	0.309 ± 0.004	86.4 ± 16.1	0.315 ± 0.016	93.9 ± 5.5	0.312 ± 0.019
40	143 ± 10	0.460 ± 0.010	140 ± 15	0.466 ± 0.018	148 ± 13	0.473 ± 0.028
50	165 ± 21	0.606 ± 0.010	161 ± 15	0.607 ± 0.011	176 ± 9	0.614 ± 0.011
60	195 ± 11	0.772 ± 0.005	195 ± 21	0.779 ± 0.015	210 ± 14	0.782 ± 0.013
70	225 ± 30	0.952 ± 0.009	226 ± 22	0.959 ± 0.039	241 ± 11	0.965 ± 0.047
80	278 ± 22	1.157 ± 0.018	280 ± 7	1.170 ± 0.037	273 ± 24	1.183 ± 0.021
90	308 ± 11	1.419 ± 0.010	310 ± 26	1.437 ± 0.026	303 ± 14	1.438 ± 0.096

[a] Relative humidity

[b] Standard deviations calculated on three batches

[c] Percentage of mass increase

Microsphere formulation conditions were optimized to produce particles with a mean diameter higher than the mesh size of collagen gel (which is known to be around 1 μm [23]), and thus considered immobile within the scaffold. Release kinetics of the model protein BSA-Rhod were assessed directly inside collagen scaffold by a CLSM-assisted technique. Results demonstrated that protein release rates can be tuned by varying microsphere formulation and scaffold composition. It was postulated that the formulation affects the initial internal porosity of microspheres, thus regulating the hindrance to the diffusion of the encapsulated protein through microspheres bulk. On the other hand, scaffold composition, as regulated by collagen/HA ratio, was found to influence mainly the onset time of protein release.

The aim of this work was to get an insight into the multiple phenomena governing protein release from PLGA microsphere-integrated collagen scaffolds. Release kinetics of BSA-Rhod from different microsphere formulations in collagen gels containing varying amounts of HA (0–2.5–5.0 mg/ml) were assessed and interpreted by evaluating the specific contribution of both microspheres and scaffold to the overall protein transport phenomena occurring in the integrated system. To this end, water absorption and degradation kinetics of PLGA microspheres in water as well as protein diffusion within the gels were studied.

It was immediately apparent from release data that both microsphere formulation and scaffold composition significantly affect BSA-Rhod release profiles (Fig. 4). This effect can be described on the basis of the two parameters introduced in data fitting, that is the time-lag t_L and the kinetic constant k (Table 2). The first accounts for the time necessary for water to penetrate into the microparticle and activate BSA-Rhod diffusion through microsphere and release, while the second gives an estimate of the overall protein release rate. As previously observed [16], microsphere formulation primarily affects protein release delay. An immediate delivery was associated to PLGA10 irrespective of HA content in the gel, while PLGA15 and PLGA20 showed an increasingly delayed release as compared to PLGA10. In addition, increasing t_L values were observed when increasing HA concentration in the collagen scaffold for the two formulations prepared at higher PLGA concentrations. Also release rates could be varied as a function of scaffold composition. In particular, in the case of PLGA10 formulation, characterized by an immediate release of the protein, release rate (i.e. k value) was found to be steadily decreasing with increasing HA concentration within the scaffold. Contrariwise, k does not substantially change for PLGA15 and PLGA20 independently upon scaffold composition, i.e. overall protein release basically occurs with the same course.

It was previously observed that release profiles of BSA-Rhod in collagen scaffolds were similar to those obtained in solution, suggesting that similar release mechanisms occur in water and collagen [16]. Thus, the effect of microsphere formulation on the main phenomena controlling protein release, that is microsphere water adsorption rate and polymer degradation kinetics, were studied in an aqueous release environment. As well known, protein release from biodegradable polyester-based devices in an aqueous milieu is governed by a combined diffusion-degradation-erosion mechanism triggered by water intrusion within the polymeric matrix [24–26]. PLGA degradation occurs in the bulk [27] by the hydrolytic cleavage of the ester bonds in the polymer backbone, which is further enhanced by the accumulation of acidic products in the polymeric bulk, thus establishing an autocatalytic degradation mechanism

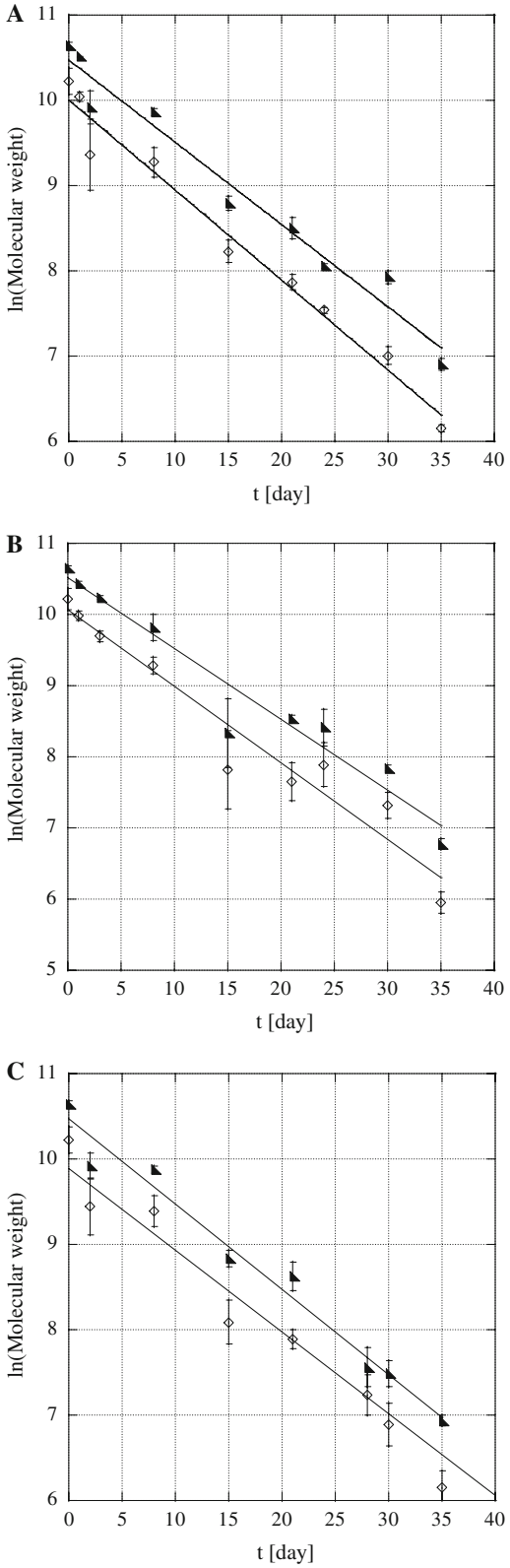

Fig. 2 Effect of microsphere formulation on PLGA degradation kinetics upon exposure to PBS (pH = 7.4). **a** PLGA10; **b** PLGA15; **c** PLGA20. (*Right angled triangle*): Weight-average molecular weights, (*diamond*): Number-average molecular weights. Data were fitted according to Eq. 1 (*Solid lines*: fitting results)

Table 2 Kinetic parameters as calculated by Eq. 4

	PLGA10			PLGA15			PLGA20		
	Coll[a]	CollHA2.5	CollHA5.0	Coll[a]	CollHA2.5	CollHA5.0	Coll[a]	CollHA2.5	CollHA5.0
k [day^{-1}] (± SD)[b]	0.616 (± 0.059)	0.224 (± 0.107)	0.103 (± 0.045)	0.107 (± 0.024)	0.097 (± 0.006)	0.105 (± 0.064)	0.163 (± 0.030)	0.131 (± 0.012)	0.160 (± 0.137)
γ_∞	0.275 (± 0.054)	0.155 (± 0.040)	0.067 (± 0.080)	0.157 (± 0.064)	0.178 (± 0.022)	0.188 (± 0.037)	0.191 (± 0.020)	0.115 (± 0.041)	0.260 (± 0.017)
t_L [day] (± SD)[b]	−0.048 (± 0.430)	0.027 (± 0.687)	0.076 (± 0.653)	0.407 (± 0.994)	1.730 (± 0.453)	1.812 (± 1.648)	4.492 (± 1.368)	5.805 (± 0.551)	8.747 (± 4.713)

[a] Data recalculated based on [16]

[b] Standard deviations calculated on three different batches

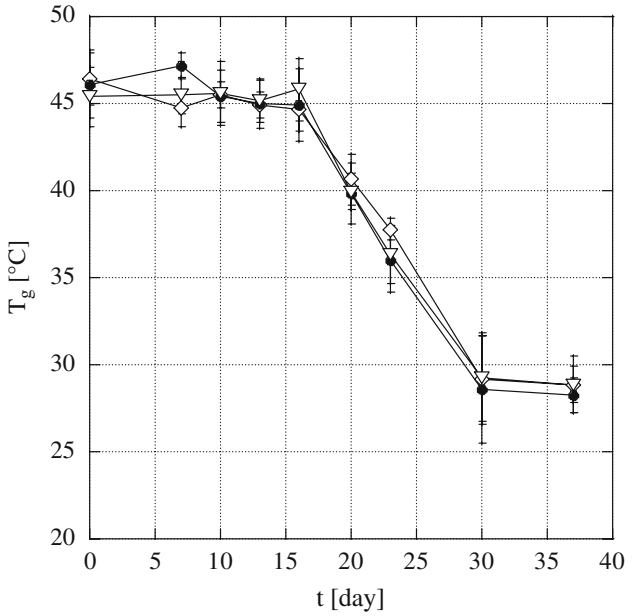

Fig. 3 Temporal trend of glass transition temperature in PBS at 37°C under gentle agitation (15 rpm) as a function of microsphere formulation. (*diamond*): PLGA10; (*circle*): PLGA15; (*inverted triangle*): PLGA20

[28, 29]. The protein is solubilized by the water intruded in microspheres and migrates through the interconnected pore network in the degrading polymer matrix [30, 31]. Release rates can be generally regulated by selecting adequate formulation conditions, such as polymer concentration in the organic phase, which affect initial hydration phase, internal morphology and erosion rate of the matrix.

It was previously observed that release profiles of BSA-Rhod in collagen scaffolds were similar to those obtained in solution by the same technique, suggesting that similar release mechanisms occur in water and collagen [16]. Thus, the effect of microsphere formulation on the main phenomena controlling protein release, that is microsphere water adsorption rate and polymer degradation kinetics were studied in an aqueous release environment.

Release onset is triggered by microsphere hydration phase and therefore depends on water transport within microspheres, which activates protein solubilization and diffusion outwards as well as polymer degradation. Water intrusion kinetics inside microspheres as evaluated by DVS highlighted that the trends of mass increase as a function of time were similar for all microsphere types, thus showing that PLGA degradation is triggered with the same velocity irrespective of the formulation variable. These results were confirmed by GPC data, which showed that the evolutions of number-average and weight-average molecular weights upon microsphere degradation are essentially superimposable for the three microsphere formulations, with randomly variable polidispersity indices (ranging from 1.30 to 2.62).

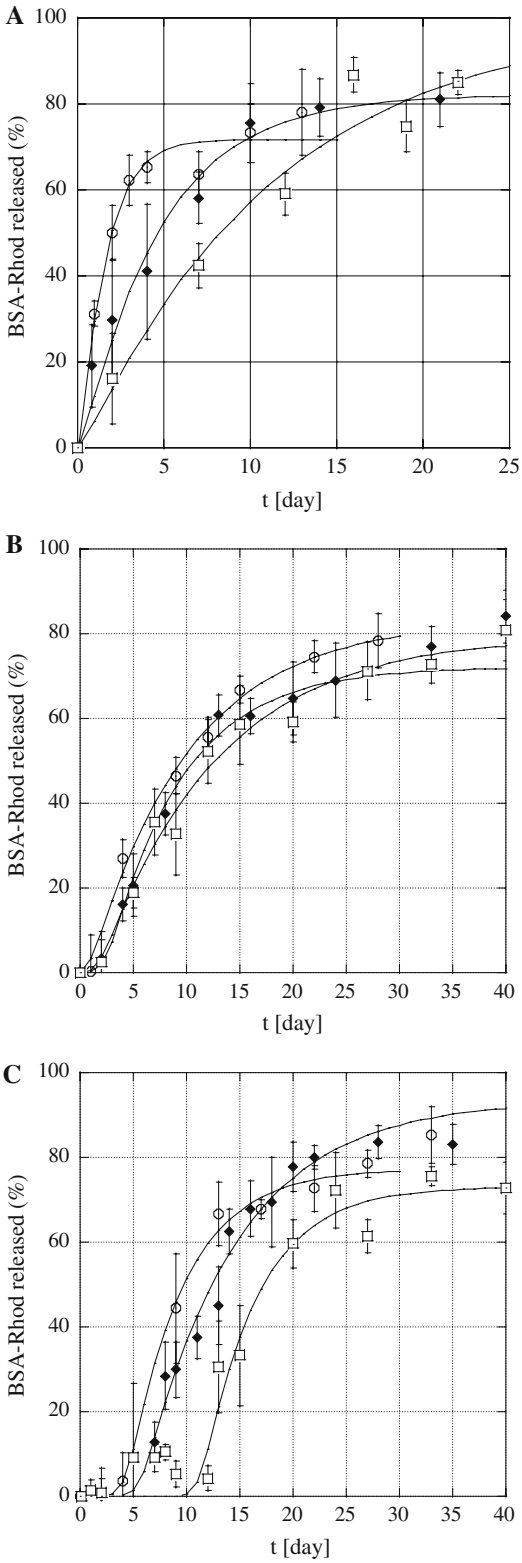

Fig. 4 In vitro protein release kinetics from PLGA microspheres as a function of microsphere formulation and hyaluronic acid content. **a** PLGA10 (data reported for comparison) [16]; **b** PLGA15; **c** PLGA20. (*Circle*): Coll1.2 scaffold; (*diamond*): CollHA2.5 scaffold; (*square*): CollHA5.0 scaffold. Data were fitted according to Eq. 4 (*Solid lines*: fitting results)

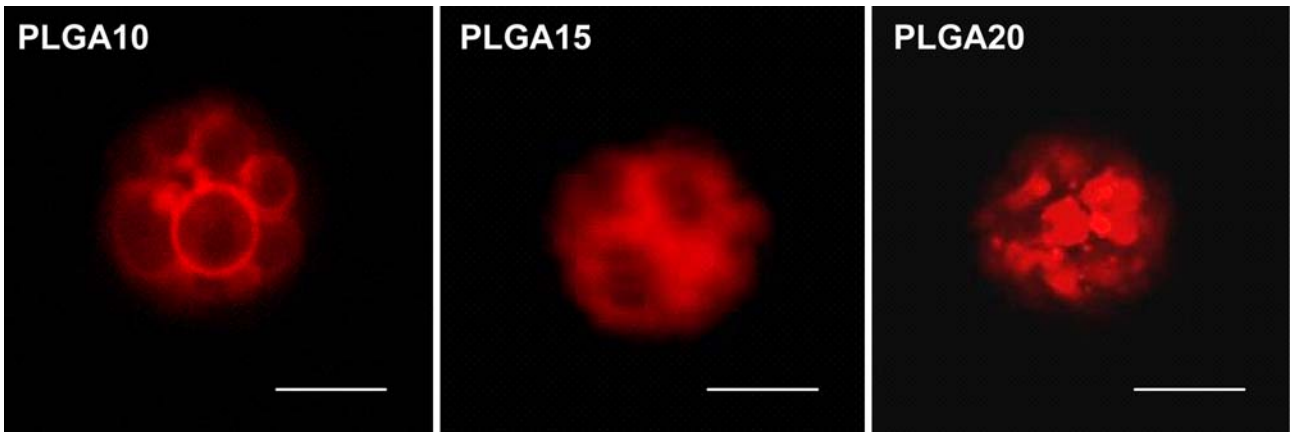

Fig. 5 Confocal images of PLGA microspheres loaded with BSA-Rhod in collagen scaffolds prior to microsphere degradation. The bar is 10 μm

Table 3 Degradation parameters calculated for PLGA microspheres

	PLGA10	PLGA15	PLGA20
$M_{w,0}^{a} \pm SD^{b}$ [kDa]	38.2 ± 3.5	40.4 ± 1.8	34.5 ± 3.2
$k_{deg,w}^{c} \pm SD^{b}$ [day^{-1}]	0.102 ± 0.006	0.102 ± 0.004	0.0961 ± 0.0071
$M_{n,0}^{d} \pm SD^{b}$ [kDa]	24.0 ± 2.8	25.0 ± 3.5	23.1 ± 4.4
$k_{deg,n}^{e} \pm SD^{b}$ [day^{-1}]	0.110 ± 0.007	0.109 ± 0.003	0.106 ± 0.008

[a] Initial weight-average molecular weight

[b] Standard deviations calculated on three batches

[c,e] Degradation constants

[d] Initial number-average molecular weight

This strongly suggests that the transport of water (which triggers polymer degradation) and of acid oligomers (which catalyze polymer degradation) are not affected by the internal microstructure of microspheres (Fig. 5). Thus, it can be assumed that microsphere internal porosity plays a role in determining protein release rate only in the early diffusive phase, when the contribution of polymer degradation is not relevant.

Once activated, protein release from microsphere-integrated scaffold will be strongly contributed by microsphere hydrolytic degradation. As underlined above, degradation studies performed in water demonstrated that PLGA degradation kinetics are not affected by the formulation variable. No significant difference in the evolution of PLGA molecular weights upon microsphere degradation was observed (Fig. 2). In each case, degrading PLGA microspheres showed a progressive loss of the spherical shape from day 15, while the external surface remained basically intact independently of formulation conditions (Fig. 1). This can be related to the progressive formation of large, randomly dispersed cavities within the microspheres [32], and indicates the occurrence of the well-known autocatalytic PLGA degradation, which is promoted in the microsphere bulk. The degraded region of the microsphere, evolving outwards, leads to an extensive loss of physical integrity of the device in 30–35 days as confirmed by a strong decrease of T_g upon time (Fig. 3), which was again similar for all formulations. The progressive molecular weight decrease of degrading microspheres resulted in a loss of mechanical properties after 30–35 days of release due to the progressive decrease in PLGA chain entanglements. This further indicates that formulation variable does not affect the changes in the mobility of PLGA molecules.

In the case of microsphere-integrated scaffolds, the chemico-physical properties of the template (e.g. hydrophilicity, composition) may also affect the release kinetics and should be taken into account. Thus, in the case of collagen/HA semi-IPNs, the presence of HA chains should be considered. Actually, HA is a twisted molecule due to the secondary hydrogen bonds along the polymer chains, which generate hydrophobic patches and therefore an expanded random coil containing extensive entanglements. Moreover, HA is an extensively swollen macromolecule and displays an extraordinary capability to sequester water [14]. DVS results achieved on microspheres in water clearly indicate that the strong dependence of t_L upon HA content of the collagen gel detected for PLGA15 and PLGA20 formulations can be attributed only to scaffold composition, i.e. HA addition. Thus, while pure collagen essentially behaves as water, the presence of increasing HA concentrations in the collagen gel is likely to produce a progressively more hindered water transport in the gel and, consequently, a progressively more delayed protein release.

Scaffold influence on release rate can be immediately gathered from FCS results (Table 4), which indicate that increasing HA amounts in the collagen gel impose increasing obstacles to macromolecular transport, likely

Table 4 Diffusion coefficients of BSA-Rhod collagen gels and collagen-HA semi-IPNs as measured by FCS

	$(D_{BSA-Rhod} \pm SD)^a \times 10^7$ [cm^2/s]
Coll	4.39 ± 0.69
CollHA2.5	2.78 ± 0.70
CollHA5.0	2.41 ± 0.44

[a] Standard deviations calculated on five batches

ascribable to a shrinkage of collagen meshes in the presence of HA [14]. Thus, the diffusional hindrances due to the steric exclusion effect imposed by HA appear to primarily govern protein delivery within collagen-based scaffolds in the case of PLGA10. It should also be underlined that in HA-free scaffold, the *k* value of PLGA10 is about 5-fold higher compared to *k* for PLGA15 and PLGA20 formulations, due to the higher superficial and internal interconnected microporosity [33] promoting protein release. Notably, protein release basically occurs with the same rate for PLGA15 and PLGA20 independently upon scaffold composition. This suggests that, for these two formulations, the transport resistance is much more significant in microspheres than in the scaffold, thus implying that microsphere erosion at the micropore level primarily governs the velocity of protein discharging. On the contrary, in the case of PLGA10, initial microporosity is high enough to allow immediate protein delivery.

Taken all together, results showed that autocatalysis is not the only mechanism governing protein release from biodegradable polymers. When microspheres are integrated in collagen gels and in collagen-HA semi-IPNs, water activity in the gel significantly contributes to protein release. While microsphere formulation primarily influences the release duration and rate, the amount of HA in the scaffold mainly influences the time necessary for release onset. Therefore, the engineering of protein release kinetics in terms of amount and microsphere discharge rate can be modulated by microsphere formulation and HA concentration in the scaffold. This allows to obtain a predetermined and possibly sequential delivery of different proteins from PLGA microspheres.

5 Conclusions

The CLSM-assisted release technique, properly associated to diffusion and degradation kinetics studies, allowed to get an insight into the factors governing protein release rate from biodegradable microspheres within collagen-based scaffolds. Results clearly indicate that polymer degradation, protein transport through degrading microsphere bulk and within the gel, together with water diffusion/sequestration in the polymer template, contribute to determine protein release kinetics. In particular, the proper manipulation of microsphere formulation and HA content within collagen-based scaffold may enable a fine engineering of protein release kinetics, meaning the presentation of correct morphogenetic factors according to a predetermined temporal sequence.

Acknowledgements The authors warmly wish to thank Dr. Ilaria De Santo for her precious advices in FCS and Dr. Lucia Sansone for her support in DVS experiments.

References

1. Hutmacher DW. Scaffold design and fabrication technologies for engineering tissues—state of the art and future perspectives. J Biomater Sci Polym Ed. 2001;12:107–24. doi:10.1163/156856201744489.
2. Tabata Y. Significance of release technology in tissue engineering. Drug Discov Today. 2005;10:1639–46. doi:10.1016/S1359-6446(05)03639-1.
3. Tabata Y. Tissue regeneration based on growth factor release. Tissue Eng. 2003;9:S5–15. doi:10.1089/10763270360696941.
4. Mikos AG, Herring SW, Ochareon P, Elisseeff J, Lu HH, Kandel R, et al. Engineering complex tissues. Tissue Eng. 2006;12:3307–39. doi:10.1089/ten.2006.12.3307.
5. Saltzman WM, Olbricht WL. Building drug delivery into tissue engineering. Nat Rev Drug Discov. 2002;1:177–86. doi:10.1038/nrd744.
6. Biondi M, Ungaro F, Quaglia F, Netti PA. Controlled drug delivery in tissue engineering. Adv Drug Deliv Rev. 2008;60:229–42. doi:10.1016/j.addr.2007.08.038.
7. Chen RR, Mooney DJ. Polymeric growth factor delivery strategies for tissue engineering. Pharm Res. 2003;20:1103–12. doi:10.1023/A:1025034925152.
8. Boontheekul T, Mooney DJ. Protein-based signaling systems in tissue engineering. Curr Opin Biotechnol. 2003;14:559–65. doi:10.1016/j.copbio.2003.08.004.
9. Tessmar JK, Göpferich AM. Matrices and scaffolds for protein delivery in tissue engineering. Adv Drug Deliv Rev. 2007;59:274–91. doi:10.1016/j.addr.2007.03.020.
10. Zhang G, Suggs LJ. Matrices and scaffolds for drug delivery in vascular tissue engineering. Adv Drug Deliv Rev. 2007;59:360–73. doi:10.1016/j.addr.2007.03.018.
11. Ungaro F, Biondi M, Indolfi L, De Rosa G, La Rotonda MI, Quaglia F, et al. Bioactivated polymer scaffolds for tissue engineering. In: Ashammakhi N, Rise RL, Sun W, editors. Topics in tissue engineering, vol II. 2005.
12. Bosman FT, Stamenkovic I. Functional structure and composition of the extracellular matrix. J Pathol. 2003;200:423–8. doi:10.1002/path.1437.
13. Reichenberger E, Olsen BR. Collagens as organizers of extracellular matrix during morphogenesis. Semin Cell Dev Biol. 1996;7:631–8. doi:10.1006/scdb.1996.0077.
14. Fraser JR, Laurent TC, Laurent UB. Hyaluronan: its nature, distribution, functions and turnover. J Intern Med. 1997;242:27–33. doi:10.1046/j.1365-2796.1997.00170.x.
15. Toole BP. Hyaluronan in morphogenesis. Semin Cell Dev Biol. 2001;12:79–87. doi:10.1006/scdb.2000.0244.
16. Ungaro F, Biondi M, D'Angelo I, Indolfi L, Quaglia F, Netti PA, et al. Microsphere-integrated collagen scaffolds for tissue engineering: effect of microsphere formulation and scaffold properties on protein release kinetics. J Control Release. 2006;113:128–36. doi:10.1016/j.jconrel.2006.04.011.

17. Xin X, Borzacchiello A, Netti PA, Ambrosio L, Nicolais L. Hyaluronic-acid-based semi-interpenetrating materials. J Biomater Sci Polym Ed. 2004;15:1223–36. doi:10.1163/1568562041753025.
18. Bass M, Van Stryland EW, Williams DR, Wolfe WL. Handbook of optics. 2nd ed, vol II. New York: McGraw-Hill Inc.; 1995.
19. McNamara KP, Nguyen T, Dumitrascu G, Ji J, Rosenzweig N, Rosenzweig Z. Synthesis, characterization, and application of fluorescence sensing lipobeads for intracellular pH measurements. Anal Chem. 2001;73:3240–6. doi:10.1021/ac0102314.
20. Haustein E, Schwille P. Fluorescence correlation spectroscopy: novel variations of an established technique. Annu Rev Biophys Biomol Struct. 2007;36:151–69. doi:10.1146/annurev.biophys.36.040306.132612.
21. Gösch M, Rigler R. Fluorescence correlation spectroscopy of molecular motions and kinetics. Adv Drug Deliv Rev. 2005;57:169–90. doi:10.1016/j.addr.2004.07.016.
22. Magde D, Elson EL, Webb WW. Fluorescence correlation spectroscopy. II. An experimental realization. Biopolymers. 1974;13:29–61. doi:10.1002/bip.1974.360130103.
23. Tranquillo R, Isenberg B. Artificial soft tissue fabrication from cell-contracted biopolymers. In: Guilak F, Butler D, Goldstein S, Mooney DJ, editors. Functional tissue engineering. New York: Springer; 2004. p. 305–317.
24. Crotts G, Park TG. Protein delivery from poly(lactic-co-glycolic acid) biodegradable microspheres: release kinetics and stability issues. J Microencapsul. 1998;15:699–713. doi:10.3109/02652049809008253.
25. Park TG. Degradation of poly(lactic-co-glycolic acid) microspheres: effect of copolymer composition. Biomaterials. 1995;16:1123–30. doi:10.1016/0142-9612(95)93575-X.
26. Grizzi I, Garreau H, Li S, Vert M. Hydrolytic degradation of devices based on poly(D,L-lactic acid) size-dependence. Biomaterials. 1995;16:305–11. doi:10.1016/0142-9612(95)93258-F.
27. Hutchinson FG, Furr BJ. Biodegradable polymers for the sustained release of peptides. Biochem Soc Trans. 1985;13:520–3.
28. Von Burkersroda F, Schedl L, Göpferich A. Why degradable polymers undergo surface erosion or bulk erosion. Biomaterials. 2002;23:4221–31. doi:10.1016/S0142-9612(02)00170-9.
29. Siepmann J, Elkharraz K, Siepmann F, Klose D. How autocatalysis accelerates drug release from PLGA-based microparticles: a quantitative treatment. Biomacromolecules. 2005;6:2312–9. doi:10.1021/bm050228k.
30. Péan JM, Venier-Julienne MC, Boury F, Menei P, Denizot B, Benoit JP. NGF release from poly(D,L-lactide-co-glycolide) microspheres. Effect of some formulation parameters on encapsulated NGF stability. J Control Release. 1998;56:175–87. doi:10.1016/S0168-3659(98)00086-8.
31. Hernadez RM, Igartua M, Gascon AR, Calvo MB, Pedraz JL. Influence of shaking and surfactants on the release of BSA from PLGA microspheres. Eur J Drug Metab Pharmacokinet. 1998;23:92–6.
32. Mollica F, Biondi M, Muzzi S, Ungaro F, Quaglia F, La Rotonda MI, et al. Mathematical modelling of the evolution of protein distribution within single PLGA microspheres: prediction of local concentration profiles and release kinetics. J Mater Sci Mater Med. 2008;19:1587–93. doi:10.1007/s10856-007-3301-5.
33. Batycky RP, Hanes J, Langer R, Edwards DA. A theoretical model of erosion and macromolecular drug release from biodegrading microspheres. J Pharm Sci. 1997;86:1464–77. doi:10.1021/js9604117.